Modulation of the Gut Microbiota Alters the Tumor-Suppressive Efficacy of Tim-3 Pathway Blockade in a Bacterial Species- and Host Factor-Dependent Manner

Bokyoung Lee
Ajou University School of Medicine and Graduate School of Medicine
Jieun Lee
Ajou University School of Medicine and Graduate School of Medicine
Min-Yeong Woo
Ajou University School of Medicine and Graduate School of Medicine
Mi Jin Lee
Ajou University School of Medicine and Graduate School of Medicine
Ho-Joon Shin
Ajou University School of Medicine and Graduate School of Medicine
Kyongmin Kim
Ajou University School of Medicine and Graduate School of Medicine
Sun Park (sinsun@ajou.ac.kr)
Ajou University School of Medicine and Graduate School of Medicine https://orcid.org/0000-0003-3254-4064

Research

Keywords: Immune Checkpoint Inhibitor, Havcr2, Cancer Immunotherapy, Antibiotics, Gut Microbiota

Posted Date: August 5th, 2020

DOI: https://doi.org/10.21203/rs.3.rs-51068/v1

Abstract

Background T cell immunoglobulin and mucin domain-containing protein-3 (Tim-3) is an immune checkpoint molecule and a potential target for anti-cancer therapy. Alterations in the tumor-suppressive efficacy of immunotherapy due to gut microbiota disturbance have been reported; however, the influence of gut microbiota on the efficacy of Tim-3 blockade is yet to be investigated. In this study, we examined whether gut microbiota manipulation altered the anti-tumor efficacy of Tim-3 blockade. The gut microbiota was manipulated by the administration of antibiotics and oral gavage of bacteria to mice.

Results Alterations in the gut microbiome were analyzed by 16S rRNA gene sequencing. Gut dysbiosis triggered by antibiotics attenuated the anti-tumor efficacy of Tim-3 blockade in both C57BL/6 and BALB/c mouse strains. Anti-tumor efficacy was restored via gut microbiota manipulation through oral gavage of fecal bacteria even as antibiotic administration continued. In the case of oral gavage of Enterococcus hirae or Lactobacillus johnsonii, the transferred bacterial species and host mouse strain were critical in determining the anti-tumor efficacy of Tim-3 blockade. Furthermore, oral bacterial gavage did not increase alpha diversity of the gut microbiota in antibiotics-treated mice but did alter microbiome composition, which was associated with restoration of anti-tumor efficacy of Tim-3 blockade.

Conclusions Our results highlight the importance of the gut microbiota in anti-cancer immunotherapy responsiveness and indicate that gut microbiota modulation may increase the efficacy of immunotherapy when concomitantly administered with antibiotics. The administered bacterial species and host factors should be considered so as to benefit from gut microbiota modulation.

Background

T cell immunoglobulin and mucin domain-containing protein-3 (Tim-3) is an immunoregulatory protein encoded by the Hepatitis A virus cellular receptor 2 (*Havcr2*) gene and is an emerging target for cancer immunotherapy. It was discovered as a molecule that distinguished T helper type 1(TH1) cells from T helper type 2 (TH2) cells [1]. However, it has been detected on the surface of exhausted $CD8^+$ T cells and on certain innate cells such as natural killer (NK) cells, monocytes, and dendritic cells [2-4]. In T cells, Tim-3 delivers inhibitory signals when its cytoplasmic tail interacts with Lnc-tim3 instead of Bat3 [5]. Tim-3 is associated with the differentiation of T cells, leading to the formation of effector T cells rather than memory T cells and has also been linked to NK cell exhaustion [6,7]. Additionally, Tim-3 impedes nucleic acid-induced activation of dendritic cells, resulting in suppression of anti-tumor immunity [8]. Increased cellular expression of Tim-3 and inverse correlation of Tim-3 expression with cancer prognosis have been observed in various cancers including hepatocellular carcinoma, B cell lymphoma and pancreatic cancer [9-11]. Blocking Tim-3 signaling decreases tumor growth in mouse models [12, 13]. Furthermore, concomitant blockade of Tim-3 and PD-1 pathways enhances tumor suppression better than blocking either pathway alone [2, 14-16]. Several mechanisms are believed to underlie the tumor-suppressive effect of Tim-3 blockade, such as decrease in regulatory T cell frequencies, functional restoration of tumor-

infiltrated T cells, increased dendritic cell recruitment to the tumor tissue, and enhanced NK cell activity [7, 13, 16-19].

The efficacy of anti-cancer therapies is influenced by gut microbiota composition [20]. Certain enteric microbial enzymes directly modulate anti-cancer nucleoside analogues: for example, enhancement of fludarabine activity by purine nucleoside phosphorylase produced by *Escherichia coli* [21]. Germ-free mice and antibiotics-treated mice exhibit diminished response to chemotherapeutic drugs, including cyclophosphamide and oxaliplatin, because their therapeutic activities depend on gut microbiota-associated T cell immune response and reactive oxygen species (ROS) production [22]. Furthermore, response to immunotherapy targeting programmed cell death-1 (PD-1) or cytotoxic T-lymphocyte antigen-4 (CTLA-4) varies with gut microbiota composition in tumor bearing mice and patients [23-25]. Moreover, manipulation of gut microbiota by oral administration of *Enterococcus hirae* enhances the efficacy of cyclophosphamide in mice [26]. However, the relationship between efficacy of Tim-3 blockade and gut microbiota composition has not been investigated. In this study, we examined whether the gut microbiota modulation influences the efficacy of Tim-3 blockade in mouse tumor models.

Methods

Cell culture

B16 melanoma cells (American Type Culture Collection (ATCC), Manassas, VA, USA) and Chinese hamster ovary-K1 (CHO, ATCC) cells were cultured in Dulbecco's modified Eagle's medium (DMEM, ThermoFisher, Carlsbad, CA, U.S.A.) containing 10% fetal bovine serum (Carpricorn Scientific, Ebsdorfergrund, Germany), 100 U/mL penicillin and 100 μg/mL streptomycin (Gibco BRL, Dublin, Ireland). CT-26 cells (provided by Dr. Kwon, Ajou University) were cultured in Roswell Park Memorial Institute (RPMI) 1640 media (GIBCO) containing 10% fetal bovine serum, 100 U/mL penicillin and 100 μg/mL streptomycin. HEK-293 T cells (provided by Dr. Kwon, Ajou University) were cultured in FreeStyle^{TM} 293 expression medium (Gibco).

Construction of expression vectors for Tim-3 blocking molecules

IgV domain of Tim-3 was amplified by PCR using primers (forward primer: 5’-CGG GGT ACC GAT TGG AAA ATG CTT ATG TGT TTG AG and reverse primer: 5’-GAA TTC TGC TTT GAT GTC TAA TTT CAG TTC) and plasmid pIRES2-EGFP-Tim3SVMhIg [19]. The Tim3 V-domain DNA segment was inserted into the pSecTag2C vector (ThermoFisher Scientific, Waltham, MA, USA) containing mouse immunoglobulin (mIgG2a) CH2CH3 with and without hinge region, and named pSecTag2C-Tim3VdIg and pSecTag2C-Tim3VmIg, respectively.

Western blotting for detection of Tim3VdIg protein

CHO cells or HEK-293 T cells were transfected with a Tim3 expression vector using Polyethylenimine (Polyscience, PA USA). After 2 days, culture supernatant was collected and loaded on the sodium dodecyl sulfate polyacrylamide gel for electrophoresis (PAGE) or non-denatured PAGE followed by transfer onto polyvinylidene difluoride membrane (Bio-Rad, Hercules, CA, USA). The membrane was incubated with anti-mouse IgG Ab conjugated with horseradish peroxidase (ZYMED® Laboratories, Invitrogen, Carlsbad, CA, USA) and then developed using an enhanced chemiluminescence kit (GE Healthcare, Little Chalfont, UK).

Production and purification of Tim3VdIg protein

HEK-293T cells ($2x10^6$/mL) were transfected with pSecTag2C-Tim-3VdIg using polyethylenimine. After 7 days, the supernatant was harvested from the culture and then Tim3VdIg protein was purified using Protein A beads (GE Healthcare, Little Chalfont, UK).

Evaluation of tumor growth

Tumor growth experiments in mice were approved by the Institutional Animal Care and Use Committee, Ajou University Medical Center (IACUC protocol #2016-0003). Six-week-old male C57BL/6 and BALB/c mice were purchased form OrientBio (Gyeonggido, Korea). Mice were maintained in specific pathogen free conditions and in separate cages according to strain and treatment. Antibiotics mixture containing 900 mg/L for ampicillin (Gold Biotechnology, Saint Louis, MO, USA), 900 mg/L for neomycin (BioVision, Milpitas, CA, USA), 900 mg/L metronidazole (BioVision, Milpitas, CA, USA), and 300 mg/L for vancomycin (Gold Biotechnology, Saint Louis, MO, USA) was provided to mice via drinking water. Drinking water was replaced every third day. Three weeks later, all mice were challenged subcutaneously with 100 μL tumor cells ($3x10^6$ cells/mL) which were B16 cells for C57LL/6 mice and CT-26 for BALB/c mice. Tim-3VdIg protein (60 μg/mouse) was intraperitoneally injected on every second day for 12 days after tumor challenge. Tumor progression was assessed every second day by determining tumor volume using the formula: tumor volume = 0.523 x tumor length x $(\text{tumor width})^2$.

Oral administration of bacteria to mice

Fecal bacteria stock was prepared by collecting feces from the large intestine of eight-week-old BALB/c and C57BL/6 mice under anaerobic condition. Feces were suspended in phosphate buffered saline (PBS) at concentration of 60 mg/mL and followed by centrifugation at 800 × *g* for 3 min. The supernatant was aliquoted for storage at -70°C until it was administered orally at an amount of 100 μL per mouse seven

times in total, once every third day starting seven days before tumor challenge to a mouse. *Lactobacillus johnsonii* (Korean Culture Center of Microorganisms) and *Enterococcus hirae* (Korean Culture Center of Microorganisms) were cultured at 37^{o}C in Brain Heart Infusion media and De Man, Rogosa, and Sharpe (MRS) agar, respectively. The bacteria were cultured to an OD of 1.8 measured at 600 nm (corresponding to 10^{9} CFU/mL) and then aliquoted and cryopreserved in 15% glycerol. Each bacterial suspension (100 µL/head) was administered to a mouse seven times in total, every third day.

Collection of gut microbiota samples and bacterial DNA sequencing

Mice were sacrificed on eighth day after tumor cell challenge to collect cecal content, which was immediately frozen at -70^{o}C for microbiome analysis. DNA was extracted from cecal samples using DNeasyPowerSoil Kit (Qiagen, Hilden, Germany) according to the manufacturer's instructions. DNA quality was assessed by gel electrophoresis and fluorometry. Sequencing libraries were constructed according to the Illumina 16S Metagenomic Sequencing Library protocols using Herculase II fusion DNA polymerase (Agilent Technologies, Santa Clara, CA) and the universal primer pair specific for the V3-V4 region of the 16S rRNA gene with Illumina adapter overhang sequences. The purified PCR product was quantified according to the qPCR Quantification Protocol Guide (KAPA Library Quantification kits for Illumina Sequencing platforms) and qualified using the TapeStation D1000 ScreenTape (Agilent Technologies, Waldbronn, Germany). Paired-end sequencing was performed with Macrogen (Seoul, Korea) using the MiSeq™ platform (Illumina, San Diego, USA).

Sequence processing and taxonomic assignment

The FLASH (Fast Length Adjustment of SHort reads, 1.2.11) program was employed to merge paired-end reads [27]. Open reference operational taxonomy unit (OTU) picking was utilized using QIIME-UCLUST and NCBI databases.

Statistics

The statistical significance of differences in tumor growth between groups was analyzed using the Student’s t-test or ANOVA with Bonferroni multiple comparison test. $p < 0.05$ indicated statistical significance. Significant differences in alpha diversity were computed using Kruskal-Wallis test with Dunn’s multiple comparison test. Significant differences in beta diversity were computed using PERMANOVA and ANOSIM. Significant differences in dispersion were determined by permDISP.

Results

Tim-3 V domain – mouse IgG Fc fusion protein dimer exerts tumor-suppressive effect

We previously reported the tumor-suppressive effect of Tim-3 blockade using Tim-3hIg fusion protein comprising of Tim-3 variable domain (V) and mucin domain linked to the Fc region of human IgG [19]. The Tim-3 V domain is sufficient to bind to its ligands. Furthermore, Tim-3 dimers may show greater stability in interacting with its ligand than Tim-3 monomers. Thus, the Tim3VdIg fusion protein, a dimer of two identical polypeptides consisting of Tim-3 V domain and mouse IgG hinge and Fc regions was produced. We first examined the expression of Tim3VdIg in the culture media of CHO cells that were transformed with the Tim3VdIg expression vector. As Tim3VdIg included the IgG hinge region (Cys-Pro-Pro-Cys-Lys-Cys-Cys-Pro) containing cysteine residues that formed disulfide bonds between two identical Tim3VIg fusion proteins, it was detected approximately as a 110 kDa band in native gels and as a band of 55 kDa monomer in denatured gels (Fig. 1A). To show the dimer formation clearly, Tim3VmIg that lacked the hinge region was compared in parallel. Both Tim3VdIg and Tim3VmIg proteins were similar in size in denaturation condition but varied in native condition. Next, we assessed the purity of Tim3VdIg produced by HEK-293T cells (Fig. 1B). Tim3VdIg was detected as a single band in SDS-PAGE. We then assessed tumor-suppressive effect of purified Tim3VdIg in C57BL/6 which were inoculated with B16 melanoma cells. Mice treated with Tim3VdIg showcased significantly decreased tumor growth as compared to control mice injected with PBS ($p<0.01$).

Oral administration of antibiotics to mice attenuates tumor-suppressive effect of Tim-3 blockade

To investigate the impact of gut microbiota modulation on the tumor-suppressive efficacy of Tim3VdIg, we examined tumor growth in mice administered with Tim3VdIg concomitantly with or without antibiotics, based on a report of gut microbiota disturbance by antibiotic treatment [28]. A mixture of ampicillin, neomycin, metronidazole, and vancomycin was given to mice via drinking water from three weeks before tumor challenge until the end of the experiment. Tumor growth was monitored in C57BL/6 and BALB/c mice after injection of B16 melanoma cells and CT-26 colon cancer cells, respectively (Fig. 1D to F). Given that immunotherapeutic efficacy may vary with age, we included 8-week-old (Fig. 1D) and 1-year-old C57BL/6 mice (Fig. 1E). Significant tumor suppression by Tim3VdIg treatment was observed in both 8 week old and 1 year old C57BL/6 and 8 week old BALB/c mice compared to their controls starting from day 12 (Fig. 1D and F) or 14 (Fig. 1E) ($P<0.001$); however, significant suppression of tumor growth by Tim3VdIg was not observed in mice treated with antibiotics except for 1 year old C57BL/6 on day 14. These results indicate that Tim3VdIg may exert tumor-suppressive effect in subjects varying in genetic background, tumor type and age, but not in subjects treated with antibiotics.

Oral administration of fecal bacteria or Enterococcus hirae restores tumor-suppressive effect of Tim-3 blockade in mice treated with antibiotics

We next analyzed the influence of gut microbiota modulation on the efficacy of Tim3VdIg to ascertain whether attenuation of the tumor-suppressive effect of Tim3VdIg in mice treated with antibiotics was a result of disturbance of gut microbiota (Fig. 2). Gut microbiota was modulated by feeding mice with fecal bacteria that were prepared from normal mouse feces, *Enterococcus hirae* or *Lactobacillus johnsonii* once every third day to antibiotics-treated mice. The tumor-suppressive effect of Tim3VdIg was consistently lost in antibiotics-treated mice. However, Tim3VdIg-induced tumor suppression was partially but significantly restored in antibiotics-treated C57BL/6 mice by oral transfer of fecal bacteria or *E. hirae* (Fig. 2A). In the case of C57BL/6 mice fed with *L. johnsonii,* tumor suppression was partially restored on days 8 and 10 (the suppression percentage was approximately 70% and 60% on days 8 and 10, respectively). However, tumor suppression was not maintained thereafter (the suppression percentage declined to the level of the group treated with antibiotics alone without bacterial feeding) (Fig. 2B). In the BALB/c group, the tumor-suppressive effect of Tim3VdIg was partially restored after oral gavage with fecal bacteria but not with *E. hirae* or *L. johnsonii* (Fig. 2C and D). These results indicate that gut microbiota modulation may affect the tumor-suppressive effect of Tim-3 blockade.

Gut microbiota composition varies with antibiotic treatment, bacterial gavage and mouse strain

To verify changes in gut microbiota of mice administered with antibiotics and bacteria, we analyzed microbiome of the cecum harvested on eighth day after tumor challenge. At that time point, antibiotics treatment had been continued and oral gavage of bacteria was performed five times in total. Read count ranged from 69012 to 106016 per sample. Rarefaction measurement of 12311 reads per sample shows sufficiently covered diverse microbiome (Fig. 3A). We compared alpha diversity, representing complexity of the microbiome within a sample using Chao1 and Shannon methods (Fig. 3B to E). As expected, alpha diversity was higher in groups not treated with antibiotics than in groups treated with antibiotics, although the statistical significance was not found in all comparisons. This may be due to the small sample size. Although bacterial feeding restored the tumor-suppressive efficacy of Tim3VdIg in antibiotics-treated mice, it did not increase alpha diversity significantly.

We next analyzed beta diversity using Bray-Curtis distance (Fig. 4). Principal coordinate analysis revealed the differences between samples treated with Tim3VdIg (indicated as B_T for C57BL/6 and C_T for BALB/c) and the samples treated with both Tim3VdIg and antibiotics (indicated as B_T/A for C57BL/6 and C_T/A for BALB/c). B_T and B_T/A were separated along PC2 whereas C_T and C_T/A were separated along PC1. The C57BL/6 groups administered with Tim3VdIg, antibiotics and bacteria (indicated as B_T/A/F for transfer of fecal bacteria and B_T/A/E for transfer of *E. hirae*) were separated from B_T and B_T/A along PC1 as well as PC2. The BALB/c samples from mice treated with Tim3VdIg, antibiotics and fecal bacteria (indicated as C_T/A/F) were separated from C_T and C_T/A along PC1, as well as from the samples from mice treated with Tim3VdIg, antibiotics and *E. hirae* (indicated as C_T/A/E) along PC1 and PC2. Notably, B_T/A/F, B_T/A/E and C_T/A/F, the groups showing restoration of anti-tumor efficacy of Tim-3VdIg, were clustered. Furthermore, C_T/A/E, in which tumor suppression was

not restored, was proximal to B_T/A. These results demonstrated clustering of groups according to whether tumor suppression was observed or not.

We next compared the microbiome composition at the phylum, class, and order levels (Fig. 5). One major bacterial population belonging to *Firmicutes* (phylum) *Clostridia* (class) *Clostridiales* (order) was observed in the B_T group, whereas in the C_T group, two major populations belonging to *Bacteroidetes* (phylum) *Bacteroidia* (class) *Bacteroidales* (order) and *Firmicutes Clostridia Clostridiales* were observed. In the B_T/A group of C57BL/6, and in all other groups of BALB/c (C_T/A, C_T/A/F and C_T/A/E), *Proteobacteria Gammaproteobacteria Enterobacterales* was predominant (except in C_T/A, in which *Verrucomicrobia Verrucomicrobiae Verrucomicrobiales* was most frequent). In B_T/A/F and B_T/A/E, there were two dominant populations, namely, *Proteobacteria Gammaproteobacteria Enterobacterales* and *Firmicutes Bacilli Lactobacillales*. These results indicated that antibiotics treatment altered microbiome drastically and that feeding of antibiotic-treated mice with bacteria did not fully reconstitute gut microbiota even though it restored the tumor-suppressive effect of Tim3VdIg.

We then analyzed the difference in microbiota composition at the species level between mouse group of the same strain to find species that account for the effect of microbiota modulation on the efficacy of Tim3VdIg (Table 1 and 2). The abundance of 45 and 41 bacterial species significantly varied in C57BL/6 and BALB/c groups, respectively. Two species *Beduini massiliensis,* and *Propionispira paucivorans* were potentially linked with the negative effect on anti-tumor efficacy of Tim3VdIg in C57BL/6 as they were observed in the T/A group but not in the T, T/A/F and T/A/E groups. The increased abundance of *Proteus alimentorum* and *Akkermansia muciniphila* in T/A/E or T/A/F relative to T/A indicated their potential role in the anti-tumor effect of Tim3VdIg in C57BL/6. In BALB/c mice, we could not identify any bacterial species whose modulation may be associated with the tumor-suppressive efficacy of Tim3VdIg. Finally, we compared the microbiota composition between Tim3VdIg-treated C57BL/6 and BALB/c mice, as the feeding with *E. hirae* enhanced tumor-suppressive efficacy of Tim3VdIg in C57BL/6 mice but not in BALB/c mice (Table 3). Among the 117 bacterial species, 10 species were significantly more abundant in C57BL/6 mice and 16 species in BALB/c mice, whereas 91 species were similarly abundant in these mouse strains. Taken together, these results demonstrate that gut microbiota varies with mouse strain, antibiotic treatment and oral transfer of bacteria, and that gut microbiota modulation affects tumor-suppressive efficacy of Tim-3 blockade.

Discussion

The Tim-3 pathway is a promising cancer immunotherapy candidate. Thus, identification of factors affecting its anti-tumor efficacy is significant. In this study, the influence of gut microbiota on tumor growth in mice injected with Tim3VdIg, a Tim-3 pathway blocking molecule, was examined and three novel findings were observed. Firstly, the anti-tumor effect of Tim3VdIg dissipated in mice treated with antibiotics. All these mice showcased gut dysbiosis. Secondly, oral transfer of bacteria restored the anti-tumor efficacy of Tim3VdIg in antibiotics-treated mice, even though their gut microbiota varied in

composition compared to mice not treated with antibiotics. Thirdly, the restorative effect of bacterial transfer on anti-tumor efficacy of Tim3VdIg varied with bacterial species and mouse strain.

Tim-3 is an immune checkpoint molecule, such as PD-1 and CTLA-4. These molecules are targets of cancer immunotherapy. In line with our results, the impact of gut microbiota on the efficacy of PD-1 and CTLA-4 pathway blockade has been reported [23, 24]. In both mice and humans, PD-1 or CTLA-4 blockade has been associated with gut microbiota composition [24, 29]. The presence of Bifidobacterium and Bacteroides species in mouse gut microbiota has been correlated with tumor suppression by PD-1 and CTLA-4 blockade, respectively [29, 30]. In patients with non-small cell lung carcinoma or renal cell carcinoma, clinical responsiveness to PD-1 blockade has been associated with *Akkermansia muciniphila* and T cell response against this species [31]. Notably, *A. muciniphila* also showcased positive correlation with the tumor-suppressive effect of Tim3VdIg in C57BL/6 mice in our study (Table 1). Along with *A. muciniphila, Proteus alimentorum* was also associated with good response to Tim3VdIg in C57BL/6 mice (Table 1). However, our study was limited by the low sample number for microbiome analysis in the case of BALB/c mice. Thus, no bacterial species was found to be significantly correlated with the tumor-suppressive effect of Tim-3VdI in this strain. Nevertheless, our results clearly demonstrate the influence of gut microbiota on the therapeutic efficacy of Tim-3 blockade.

Although the mice were continuously treated with antibiotics, oral gavage of bacteria successfully restored the efficacy of Tim3VdIg. Many studies have reported that administration of antibiotics causes transient gut dysbiosis, with the duration of dysbiosis depending on the duration of antibiotics administration and frequency of antibiotics courses, as well as bacterial coverage of the antibiotics [28, 32]. However, it was difficult to find a report regarding microbiota recovery by concomitant oral administration of bacteria during a course of antibiotics. Cancer patients may have to consume antibiotics either just before or during their immunotherapy as a treatment for concomitant infection. They may also be administered as a preventive measure for medical procedures such as cystoscopy in bladder cancer patients, in order to monitor recurrence of a tumor. We evaluated the influence of oral administration of bacteria on the efficacy of Tim3VdIg in mice concomitantly being administered antibiotics and discovered the favorable effect of bacterial administration on the efficacy of Tim3VdIg. Although neither gut microbiota diversity or composition was fully recovered in mice by oral bacterial administration (Fig. 3 and 4), alterations in gut microbiota composition were observed (Fig. 4 and 5). Furthermore, clustering of mouse groups according to tumor suppression and oral bacterial administration during the principal coordinate analysis of the microbiome suggests that presence or absence of principal bacterial species may affect the efficacy of Tim3VdIg more than the microbiome alpha diversity does. A recent study reported that 28% of patients with a tumor took antibiotics within 60 days before or 30 days after the first treatment of PD-1 inhibitor, and their outcomes were poor compared to patients who did not take antibiotics[31]. Our results indicate that concomitant modulation of gut microbiota with anti-tumor immunotherapy may be beneficial in such cases.

Recovery of Tim3VdIg efficacy by oral administration of bacteria relied on transferred bacterial species and the host strain. Transfer of *E. hirae* but not *L. johnsonii* stably upregulated the efficacy of Tim-3

blockade in C57BL/6 mice. Similar to our results, *E. hirae* but not *L. johnsonii* improved the efficiency of cyclophosphamide in C57BL/6 mice pretreated with antibiotics [26]. However, we should mention that *L. johnsonii* is deficient in mice that are more susceptible to cancers and can activate NK cells. It can also lower the kynurenine-tryptophan ratio, which is associated with immune suppression in healthy humans [33-35]. *E. hirae* crosses the small intestinal epithelial barrier, migrates to peripheral lymphoid organs, and upregulates the cytotoxic/regulatory T cell ratio in tumor tissues [26]. Additionally, lipoteichoic acid from *E. hirae* elicits release of several cytokines including tumor necrosis factor-α in mice [36]. Furthermore, *E. hirae*-specific T cell responses are correlated with favorable outcomes in cancer patients [37]. Contrary to data obtained from C57BL/6 mice, BALB/c mice did not benefit from administration of *E. hirae*. Notably, administration of their own fecal bacteria induced a greater restoration of the anti-tumor efficacy of Tim3Vdlg in C57BL/6 mice than in BALB/c mice (70-80% vs 40-50% suppression). The cause of this variation is unknown. It may be attributed to variations in intestinal response to transferred bacteria, immunologic response, and gut microbiota composition between C57BL/6 and BALB/c mice. Differential gene expression in the intestine of BALB/c after probiotic treatment compared to that in C57LL/6 [38], propensity towards TH1- and TH2- dominant response in C57BL/6 and BALB/c, respectively [39, 40], and our results showing difference in gut microbiome between C57BL/6 and BALB/c support these hypotheses (Table 3). These host factors may interact to determine the impact of gut microbiota modulation on the tumor-suppressive activity of Tim-3 blockade.

Conclusions

Our results emphasize the critical role of gut microbiota in cancer immunotherapy involving Tim-3 pathway blockade and indicate the beneficial effect of gut microbiota modulation on tumor suppression even during the continuous antibiotics administration. Further research will help ascertain the appropriate modulation of gut microbiota via appropriate bacterial selection, taking host factors into consideration.

List Of Abbreviations

CHO, Chinese hamster ovary-K1; CTLA-4, Cytotoxic T-lymphocyte antigen 4;

Havcr2, Hepatitis A virus cellular receptor 2; NK, natural killer;

PAGE, polyacrylamide gel for electrophoresis; PBS, phosphate buffered saline;

PD-1, programmed cell death-1; ROS, Reactive oxygen species;

TH1, T helper type 1; TH2, T helper type 2;

Tim-3, T cell immunoglobulin and mucin domain-containing protein-3

Declarations

Ethics approval

This study was approved by the Institutional Animal Care and Use Committee, Ajou University Medical Center (IACUC protocol #2016-0003).

Consent for publication

Not applicable

Availability of data and materials

The datasets supporting the conclusions of this article are included within the article and its additional files.

Competing interests

The authors have no conflict of interest to declare.

Funding

This work was supported by the Intramural Research Fund of Ajou University Medical Center (2020).

Authors' Contributions

B Lee, J Lee, M-Y Woo and MJ Lee performed all experiments and statistical analysis of all data and produced figures. K Kim critically reviewed the manuscript. S Park conceived the study, designed the experiments and wrote the manuscript. All authors read and approved the final manuscript.

Acknowledgements

We thank Office of Biostatistics, Institute of Medical Sciences, Ajou University School of Medicine for the statistical consult.

References

1. Monney L, Sabatos CA, Gaglia JL, Ryu A, Waldner H, Chernova T, et al. Th1-specific cell surface protein Tim-3 regulates macrophage activation and severity of an autoimmune disease. Nature. 2002;415:536-41.
2. Zhou Q, Munger ME, Veenstra RG, Weigel BJ, Hirashima M, Munn DH, et al. Coexpression of Tim-3 and PD-1 identifies a CD8+ T-cell exhaustion phenotype in mice with disseminated acute myelogenous leukemia. Blood. 2011;117:4501-10.
3. Gleason MK, Lenvik TR, McCullar V, Felices M, O'Brien MS, Cooley SA, et al. Tim-3 is an inducible human natural killer cell receptor that enhances interferon gamma production in response to galectin-9. Blood. 2012;119:3064-72.
4. Nakayama M, Akiba H, Takeda K, Kojima Y, Hashiguchi M, Azuma M, et al. Tim-3 mediates phagocytosis of apoptotic cells and cross-presentation. Blood. 2009;113:3821-30.
5. Ji J, Yin Y, Ju H, Xu X, Liu W, Fu Q, et al. Long non-coding RNA Lnc-Tim3 exacerbates CD8 T cell exhaustion via binding to Tim-3 and inducing nuclear translocation of Bat3 in HCC. Cell death & disease. 2018;9:478.
6. Avery L, Filderman J, Szymczak-Workman AL, Kane LP. Tim-3 co-stimulation promotes short-lived effector T cells, restricts memory precursors, and is dispensable for T cell exhaustion. Proceedings of the National Academy of Sciences of the United States of America. 2018;115:2455-60.
7. Gallois A, Silva I, Osman I, Bhardwaj N. Reversal of natural killer cell exhaustion by TIM-3 blockade. Oncoimmunology. 2014;3:e946365.
8. Chiba S, Baghdadi M, Akiba H, Yoshiyama H, Kinoshita I, Dosaka-Akita H, et al. Tumor-infiltrating DCs suppress nucleic acid-mediated innate immune responses through interactions between the receptor TIM-3 and the alarmin HMGB1. Nature immunology. 2012;13:832-42.
9. Huang X, Bai X, Cao Y, Wu J, Huang M, Tang D, et al. Lymphoma endothelium preferentially expresses Tim-3 and facilitates the progression of lymphoma by mediating immune evasion. J Exp Med. 2010;207:505-20.
10. Li H, Wu K, Tao K, Chen L, Zheng Q, Lu X, et al. Tim-3/galectin-9 signaling pathway mediates T-cell dysfunction and predicts poor prognosis in patients with hepatitis B virus-associated hepatocellular carcinoma. Hepatology (Baltimore, Md). 2012;56:1342-51.
11. Shindo Y, Hazama S, Suzuki N, Iguchi H, Uesugi K, Tanaka H, et al. Predictive biomarkers for the efficacy of peptide vaccine treatment: based on the results of a phase II study on advanced pancreatic cancer. Journal of experimental & clinical cancer research : CR. 2017;36:36.
12. Kikushige Y, Shima T, Takayanagi S, Urata S, Miyamoto T, Iwasaki H, et al. TIM-3 is a promising target to selectively kill acute myeloid leukemia stem cells. Cell stem cell. 2010;7:708-17.
13. Ngiow SF, von Scheidt B, Akiba H, Yagita H, Teng MW, Smyth MJ. Anti-TIM3 antibody promotes T cell IFN-γ-mediated antitumor immunity and suppresses established tumors. Cancer research. 2011;71:3540-51.
14. Sakuishi K, Apetoh L, Sullivan JM, Blazar BR, Kuchroo VK, Anderson AC. Targeting Tim-3 and PD-1 pathways to reverse T cell exhaustion and restore anti-tumor immunity. J Exp Med. 2010;207:2187-

94.

15. Koyama S, Akbay EA, Li YY, Herter-Sprie GS, Buczkowski KA, Richards WG, et al. Adaptive resistance to therapeutic PD-1 blockade is associated with upregulation of alternative immune checkpoints. Nature communications. 2016;7:10501.
16. Pfannenstiel LW, Diaz-Montero CM, Tian YF, Scharpf J, Ko JS, Gastman BR. Immune-Checkpoint Blockade Opposes CD8(+) T-cell Suppression in Human and Murine Cancer. Cancer immunology research. 2019;7:510-25.
17. de Mingo Pulido A, Gardner A, Hiebler S, Soliman H, Rugo HS, Krummel MF, et al. TIM-3 Regulates CD103(+) Dendritic Cell Function and Response to Chemotherapy in Breast Cancer. Cancer cell. 2018;33:60-74 e6.
18. da Silva IP, Gallois A, Jimenez-Baranda S, Khan S, Anderson AC, Kuchroo VK, et al. Reversal of NK-cell exhaustion in advanced melanoma by Tim-3 blockade. Cancer immunology research. 2014;2:410-22.
19. Lee MJ, Woo MY, Heo YM, Kim JS, Kwon MH, Kim K, et al. The inhibition of the T-cell immunoglobulin and mucin domain 3 (Tim3) pathway enhances the efficacy of tumor vaccine. Biochemical and biophysical research communications. 2010;402:88-93.
20. Helmink BA, Khan MAW, Hermann A, Gopalakrishnan V, Wargo JA. The microbiome, cancer, and cancer therapy. Nature medicine. 2019;25:377-88.
21. Hong JS, Waud WR, Levasseur DN, Townes TM, Wen H, McPherson SA, et al. Excellent in vivo bystander activity of fludarabine phosphate against human glioma xenografts that express the escherichia coli purine nucleoside phosphorylase gene. Cancer research. 2004;64:6610-5.
22. Viaud S, Daillere R, Boneca IG, Lepage P, Langella P, Chamaillard M, et al. Gut microbiome and anticancer immune response: really hot Sh*t! Cell Death Differ. 2015;22:199-214.
23. Chaput N, Lepage P, Coutzac C, Soularue E, Le Roux K, Monot C, et al. Baseline gut microbiota predicts clinical response and colitis in metastatic melanoma patients treated with ipilimumab. Ann Oncol. 2017;28:1368-79.
24. Gopalakrishnan V, Spencer CN, Nezi L, Reuben A, Andrews MC, Karpinets TV, et al. Gut microbiome modulates response to anti-PD-1 immunotherapy in melanoma patients. Science (New York, NY). 2018;359:97-103.
25. Matson V, Fessler J, Bao R, Chongsuwat T, Zha Y, Alegre ML, et al. The commensal microbiome is associated with anti-PD-1 efficacy in metastatic melanoma patients. Science (New York, NY). 2018;359:104-8.
26. Daillere R, Vetizou M, Waldschmitt N, Yamazaki T, Isnard C, Poirier-Colame V, et al. Enterococcus hirae and Barnesiella intestinihominis Facilitate Cyclophosphamide-Induced Therapeutic Immunomodulatory Effects. Immunity. 2016;45:931-43.
27. Magoc T, Salzberg SL. FLASH: fast length adjustment of short reads to improve genome assemblies. Bioinformatics. 2011;27:2957-63.
28. Ianiro G, Tilg H, Gasbarrini A. Antibiotics as deep modulators of gut microbiota: between good and evil. Gut. 2016;65:1906-15.

29. Vetizou M, Pitt JM, Daillere R, Lepage P, Waldschmitt N, Flament C, et al. Anticancer immunotherapy by CTLA-4 blockade relies on the gut microbiota. Science (New York, NY). 2015;350:1079-84.
30. Sivan A, Corrales L, Hubert N, Williams JB, Aquino-Michaels K, Earley ZM, et al. Commensal Bifidobacterium promotes antitumor immunity and facilitates anti-PD-L1 efficacy. Science (New York, NY). 2015;350:1084-9.
31. Routy B, Le Chatelier E, Derosa L, Duong CPM, Alou MT, Daillere R, et al. Gut microbiome influences efficacy of PD-1-based immunotherapy against epithelial tumors. Science (New York, NY). 2018;359:91-7.
32. Manichanh C, Reeder J, Gibert P, Varela E, Llopis M, Antolin M, et al. Reshaping the gut microbiome with bacterial transplantation and antibiotic intake. Genome Res. 2010;20:1411-9.
33. Yamamoto ML, Maier I, Dang AT, Berry D, Liu J, Ruegger PM, et al. Intestinal bacteria modify lymphoma incidence and latency by affecting systemic inflammatory state, oxidative stress, and leukocyte genotoxicity. Cancer research. 2013;73:4222-32.
34. Marcial GE, Ford AL, Haller MJ, Gezan SA, Harrison NA, Cai D, et al. Lactobacillus johnsonii N6.2 Modulates the Host Immune Responses: A Double-Blind, Randomized Trial in Healthy Adults. Frontiers in immunology. 2017;8:655.
35. Haller D, Serrant P, Granato D, Schiffrin EJ, Blum S. Activation of human NK cells by staphylococci and lactobacilli requires cell contact-dependent costimulation by autologous monocytes. Clinical and diagnostic laboratory immunology. 2002;9:649-57.
36. Takada H, Kawabata Y, Arakaki R, Kusumoto S, Fukase K, Suda Y, et al. Molecular and structural requirements of a lipoteichoic acid from Enterococcus hirae ATCC 9790 for cytokine-inducing, antitumor, and antigenic activities. Infection and immunity. 1995;63:57-65.
37. Rong Y, Dong Z, Hong Z, Jin Y, Zhang W, Zhang B, et al. Reactivity toward Bifidobacterium longum and Enterococcus hirae demonstrate robust CD8(+) T cell response and better prognosis in HBV-related hepatocellular carcinoma. Experimental cell research. 2017;358:352-9.
38. Mariman R, Tielen F, Koning F, Nagelkerken L. The Probiotic Mixture VSL#3 Has Differential Effects on Intestinal Immune Parameters in Healthy Female BALB/c and C57BL/6 Mice. The Journal of nutrition. 2015;145:1354-61.
39. Yang F, Wang D, Li Y, Sang L, Zhu J, Wang J, et al. Th1/Th2 Balance and Th17/Treg-Mediated Immunity in relation to Murine Resistance to Dextran Sulfate-Induced Colitis. Journal of immunology research. 2017;2017:7047201.
40. Yasuda Y, Shimoda T, Uno K, Tateishi N, Furuya S, Yagi K, et al. The effects of MPTP on the activation of microglia/astrocytes and cytokine/chemokine levels in different mice strains. Journal of neuroimmunology. 2008;204:43-51.

Tables

Tables provided as Supplementary Files

Figures

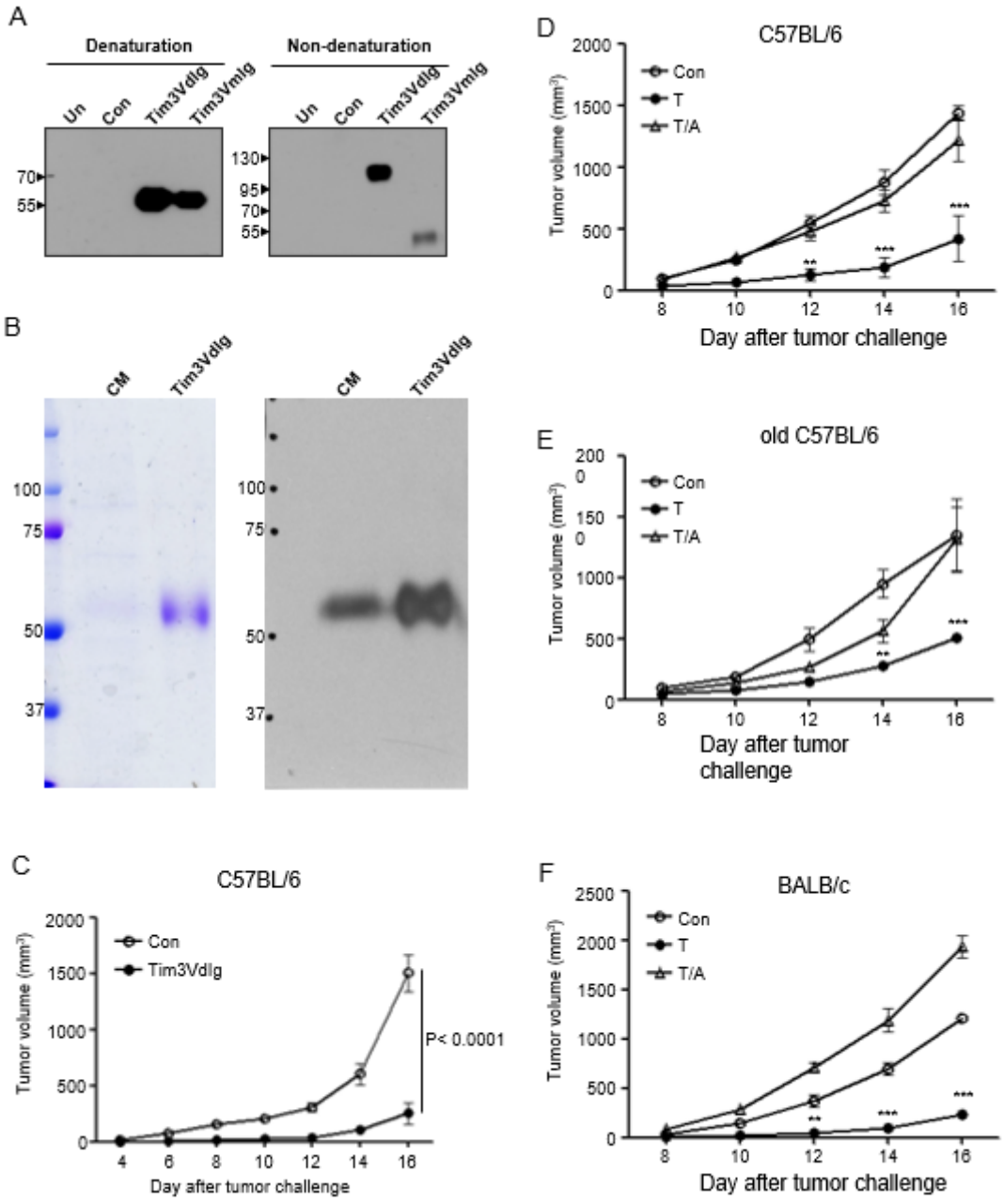

Figure 1

Antibiotic administration hinders the tumor-suppressive effect of Tim3Vdlg in two different tumor mouse models. (A) Tim3Vdlg is expressed as a dimer linked with disulfide bonds between identical polypeptides consisting of Tim-3 V domain and mouse IgG2a hinge-Fc domain. The culture supernatants of untransfected CHO cells (Un), and CHO cells transfected with pSecTag2C (Con), pSecTag2C-Tim3Vdlg or pSecTag2C-Tim3Vmlg were analyzed using Western blotting in both native and denatured conditions. Tim3Vmlg is devoid of the IgG2a hinge region of Tim3Vdlg. (B) Tim3Vdlg purified from culture media of transfected HEK-293F cells was examined using SDS-PAGE (Left) and western blotting (Right). (C) Tumor

growth in mice injected with PBS (Con, n=4) or Tim3Vdlg (60 μg/head, n=4) five times, once every second day after B16 melanoma challenge (3 x 105). Tumor growth in 8-week (D) or 1-year (E) old C57BL/6 mice injected with B16 cells (3 x 105). Tumor growth in 8-week-old BALB/c mice (F) injected with CT-26 cells (3 x 105). Tim3Vdlg was injected five times, once every second day after tumor challenge to the mouse in two groups, one of which was orally administered with antibiotics (T/A) and the other was not (T). Control group (Con) was treated with PBS. Data are represented as mean ± standard deviation. (n = 3 to 8 per group). **P<0.01, ***P<0.001 vs Con.

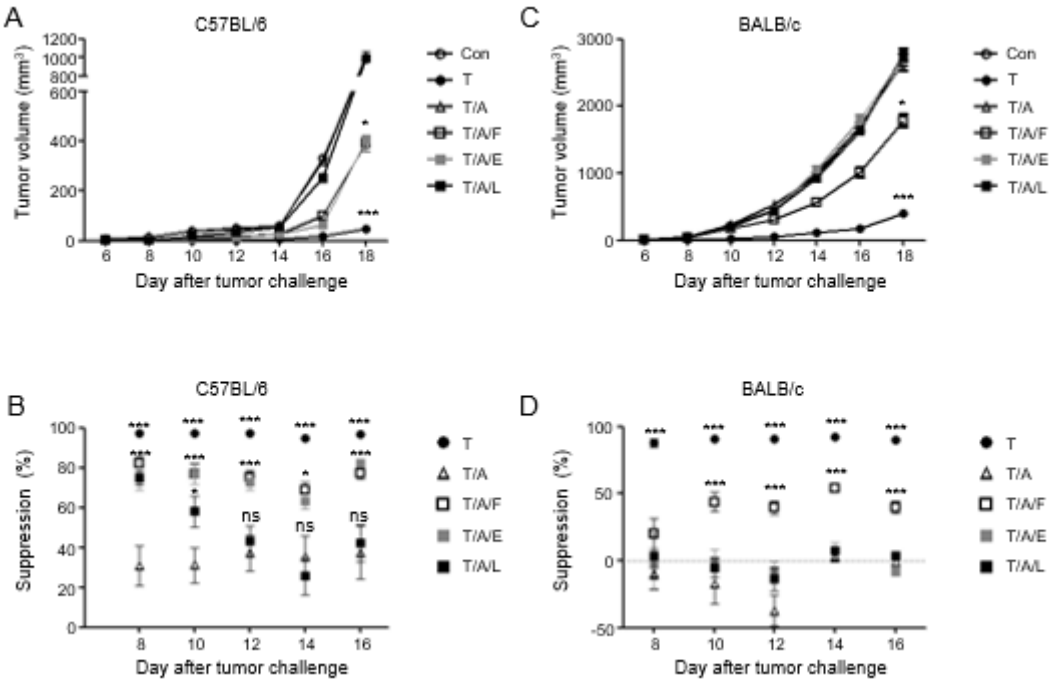

Figure 2

Bacterial gavage restores Tim3Vdlg efficacy in antibiotics-treated mice depending on bacterial species and mouse strain. Tumor growth in C57BL/6 (A) and BALB/c (C) injected with B16 melanoma cells and CT-26 cells, respectively. Control group (Con, 8 and 4 heads for C57BL/6 and BALB/c, respectively) was injected with PBS and other groups were injected with Tim3Vdlg five times, once every second day after tumor challenge. Antibiotics were administered orally. Bacteria were administered orally to the mice two times before and three times after tumor challenge. T: Tim3Vdlg treatment alone (9 and 10 heads for C57BL/6 and BALB/c, respectively). T/A: Tim3Vdlg and antibiotic treatment (10 and 9 heads for C57BL/6 and BALB/c, respectively). T/A/F: Treatment with Tim3Vdlg, antibiotics and fecal bacteria (10 and 9 heads for C57BL/6 and BALB/c, respectively). T/A/E: Treatment with Tim3Vdlg, antibiotics and Enterococcus hirae (7 and 6 heads for C57BL/6 and BALB/c, respectively). T/A/L: Treatment with Tim3Vdlg, antibiotics and Lactobacillus johnsonii (7 and 6 heads for C57BL/6 and BALB/c, respectively). Tumor suppression (C and D) was calculated as (1 – tumor volume of each mouse relative to mean tumor volume of control group) x 100. Data represent mean ± standard deviation of two independent experiments. * P<0.05, **P<0.01, ***P<0.001 vs Con or T/A.

Figure 3

Figure 3 not provided

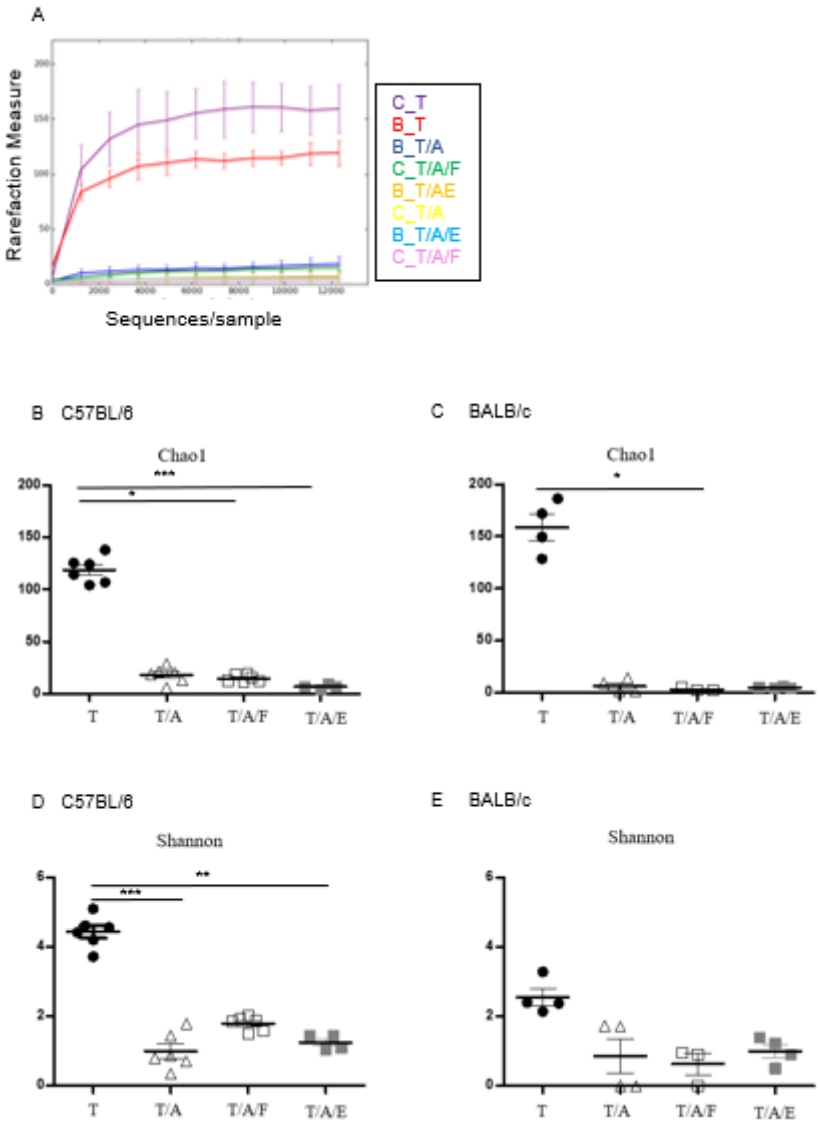

Figure 4

Bacterial oral administration does not increase the alpha diversity of the microbiome in antibiotics-treated mice. Microbiome was analyzed by 16S rDNA V3V4 sequencing using cecal content obtained from mice on the 8th day after tumor challenge. (A) Rarefaction measure after adjusting the read number of each sample by subsampling. (B-E) Alpha diversity determined by Chao1 or Shannon method. Each symbol represents each sample. C_T and B_T: BALB/c and C57BL/6 treated with Tim3Vdlg alone, respectively; C_T/A and B_T/A: BALB/c and C57BL/6 treated with Tim3Vdlg and antibiotics; C_T/A/F and B_T/A/F: BALB/c and C57BL/6 treated with Tim3Vdlg, antibiotics and fecal bacteria, C_T/A/E and B__T/A/E: BALB/c and C57BL/6 treated with Tim3Vdlg, antibiotics and Enterococcus hirae. Data represent mean ± standard deviation. * P<0.05, **P<0.01, ***P<0.001.

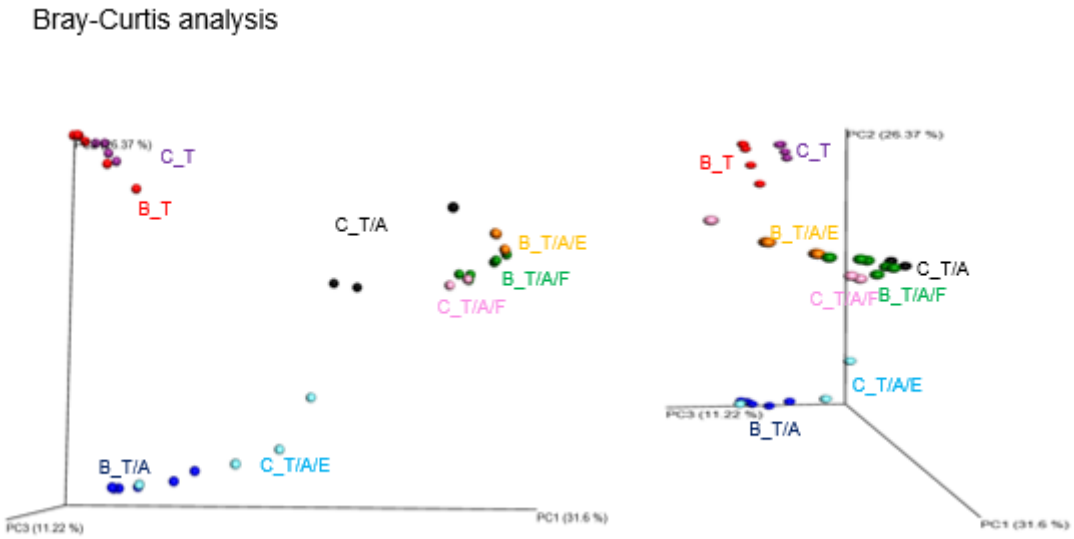

Figure 5

Beta diversity separates samples according to treatment type and mouse strain. Principal coordinate analysis of microbiome samples using Bray-Curtis distance. Microbiome was analyzed in cecal content obtained from mice on the 8th day after tumor challenge and the indicated treatment. Each symbol represents each sample. C_T and B_T: BALB/c and C57BL/6 treated with Tim3Vdlg alone, respectively; C_T/A and B_T/A: BALB/c and C57BL/6 treated with Tim3Vdlg and antibiotics; C_T/A/F and B_T/A/F: BALB/c and C57BL/6 treated with Tim3Vdlg, antibiotics and fecal bacteria, C_T/A/E and B__T/A/E: BALB/c and C57BL/6 treated with Tim3Vdlg, antibiotics and Enterococcus hirae. P = 0.001 via PERMANOVA, p = 0.013 via permDISP, R=0.813, P=0.001 via ANOSIM.

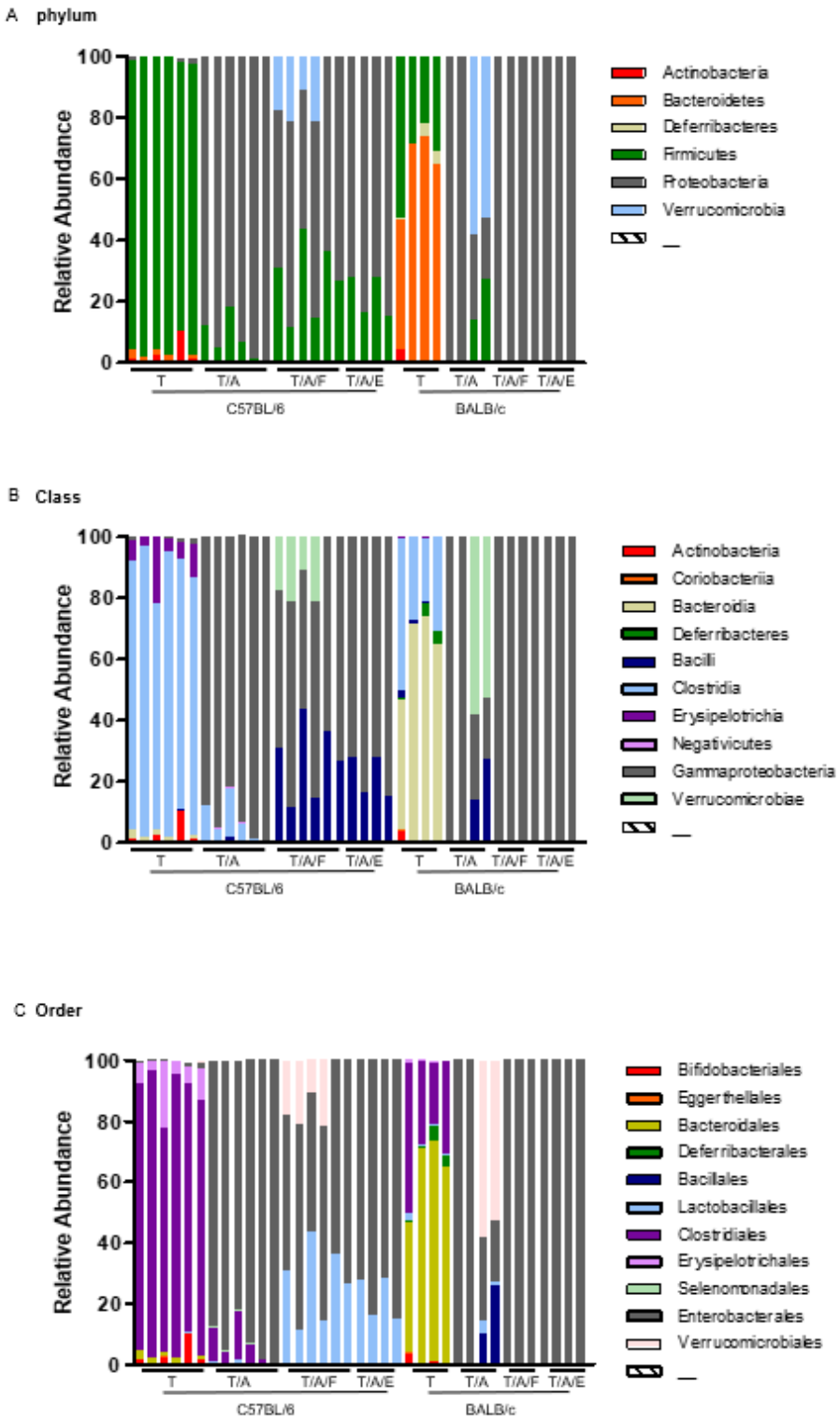

Figure 6

Relative bacterial abundance across mouse strains and treatments. Relative bacterial abundance at the phylum level (A), class level (B) and order level (C). Each bar represents each sample. T: treatment with Tim3Vdlg alone; T/A: treatment with Tim3Vdlg and antibiotics; T/A/F: treatment with Tim3Vdlg, antibiotics and fecal bacteria; T/A/E: treatment with Tim3Vdlg, antibiotics and Enterococcus hirae.

Supplementary Files

This is a list of supplementary files associated with this preprint. Click to download.

- Table1.docx
- Table2.docx
- Table3.docx
- Taxonomyabundancecount.xlsx
- OTUBLAST.xlsx
- otusrepfasta.txt